Intramolecular motions in a series of crystalline benzylammonium bromides and dibenzylamines studied by CP/MAS NMR

Frank. G. Riddell * and Martin Rogerson

School of Chemistry, The University of St Andrews, St Andrews, UK KY16 9ST

A series of 15 compounds including ammonium bromides containing one or two benzyl groups with H, methyl, isopropyl, *tert*-butyl and *tert*-amyl substituents and dibenzylamine with *N*-isopropyl-, *N*-*tert*-butyl- and *N*-*tert*-amyl substituents have been synthesised and studied by CP/MAS NMR. The results of dynamic NMR studies on the solids suggest that there is a dramatically wide range of molecular motions occurring in this simple series of compounds. A combination of 2D CPEXSY, dynamic line shape analyses and $T_{1\rho}$ measurements reveals the considerable extent of intramolecular group motions including rotations of methyl, *tert*-butyl, *tert*-amyl and phenyl groups. Rates of rotation and activation parameters for these molecular motions are derived where appropriate. In the case of benzyl-*tert*-butylammonium bromide, where two independent molecules of the compound exist in the asymmetric unit it is shown that the independent processes of *tert*-butyl rotation in the two molecules have vastly different activation energies that differ by *ca.* 16 kJ mol^{-1}. The extent of the motions observed suggests that commonly held prejudices about the rigidity of molecules in crystalline solids need revising.

Introduction

The importance in chemistry of molecular motions in crystalline solids was recognised over two decades ago when Paul and Curtin pointed out that the first step in many solid state chemical reactions should involve molecular loosening, and they showed examples where substantial molecular motion was needed for solid state reactions to occur.[1]

Despite this, there is a common, if unspoken prejudice amongst many chemists, that molecules in solids are fairly firmly held in place by their neighbours in the crystal lattice. This idea was expressed by Gavezzotti and Simonetta in 1982:[2] 'A common view among chemists, and even crystallographers, is that a molecular crystal is made up of frozen chemical entities that can at most undergo very small translational and librational motions. This is because most of the solid state investigation techniques, as well as theoretical models for the interpretation of their results, see the molecules in such a way.' This view is still widely held even today. Gavezzotti and Simonetta continued by suggesting that there was reason to suspect that the number of cases of large amplitude molecular motion in molecular crystals '... might be higher than is actually reported, given the fact that many investigators regard large molecular motions in crystals as an unlikely nuisance.'

Although many chemists now recognise that segmental motions take place in solid polymers, and that in plastic crystals or crystalline molecules of high symmetry such as benzene, rotations of whole molecules occur, the comments of Gavezzotti and Simonetta still have some currency. Molecules with irregular shapes or strong ionic interactions would not be expected by many chemists, even today, to display large amplitude segmental motions. This view is reinforced by the (static) pictures displayed of the results of X-ray diffraction studies.

In fact, although molecular motions can be demonstrated by X-ray diffraction techniques it is not the most effective method for doing this. NMR spectroscopy, by contrast, is ideally suited for measurements of molecular dynamics, particularly in solids, where a wide range of methods is available for such investigations.[3] We and others have shown that CP/MAS NMR methods can be used to study intramolecular motions.[3-15] Although CP/MAS NMR methods for this are extremely powerful they seem to be underemployed. We demonstrate in this paper, by examining a simple series of compounds that are ionic and of irregular shape, that there is an enormous variety of large amplitude molecular motions in molecular crystals that can be unravelled by solid state CP/MAS NMR techniques.

Our guiding principle in searching for such motions has been that those motions that cause the least distress to the crystal lattice should be the most readily observed by NMR methods.[4] Accordingly, most of our preliminary experiments have been performed on *tert*-butyl derivatives. The *tert*-butyl group in **1** shows dynamic line shape changes in both solid and solution states that are consistent with a *tert*-butyl group rotation.[4] The barrier to *tert*-butyl rotation is about 3 kcal mol^{-1} higher in the solid state than in solution. The additional activation energy in the solid was attributed to the stronger, directional interactions of the *tert*-butyl group with neighbouring molecules in the solid than with mobile solvent molecules in solution.

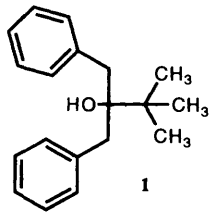

1

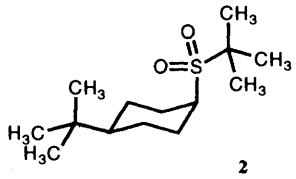

2

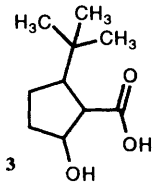

3

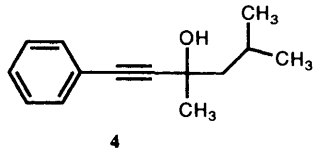

4

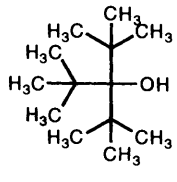

5

An extension of this work to the compound with two *tert*-butyl groups **2** showed that ^{13}C $T_{1\rho}$ measurements could be used in conjunction with dynamic line shape changes, greatly extending the rate range over which such measurements can be

made.[5] This work also showed that the two independent *tert*-butyl groups had different activation parameters for rotation. We have also recently used these methods to examine the rates of rotation of the *tert*-butyl group in two different phases of the same compound **3**.[6] This more recent piece of work has shown considerable differences in activation parameters for the same process in the same molecule in different solid phases.

Other uses of CP/MAS methods for dynamic studies in solids include a study of the phenyl rotation in **4**.[7] We have produced a preliminary report of the activation energy for methyl rotation in one of the compounds included in this paper.[8] Other reports of the rotational barrier for phenyl groups in crystalline penicillins,[9] of slowing of *tert*-butyl and methyl group rotations in **5**[10] and of dynamic spectral changes arising from pseudorotations and hydrogen bond shifts in five-membered rings[11,12] have also appeared recently.

A variety of CP/MAS NMR methods for the study of dynamic processes in solids is available.[3] The general rule is that when the frequency of the molecular motion is similar to that of an NMR interaction effects are observable in the spectrum. Rates measurable by dynamic line shape changes are comparable to the chemical shift difference and typically fall into the range 10^2–10^4 s^{-1}. Rates measurable by $T_{1\rho}$ measurements can be made when the rate of the molecular motion is similar to the precessional frequency of the nuclei in the spin locking field, typically 50–100 kHz.[5,14] Such rates typically extend from *ca.* 10^4 to as high as 10^7 s^{-1}. Similar, but not identical, is the method of so called maximum dipolar broadening.[15] This occurs when the rate of the incoherent molecular motion is similar to and so interferes with the coherent precessional frequency of the dipolar (^{1}H) decoupling field. This gives a single rate at the precessional frequency of the ^{1}H nuclei in the decoupling field. It should be noted that, when performing $T_{1\rho}$ measurements, if the ^{13}C spin lock field and the decoupler power are the same as during the Hartman Hahn condition, maximum dipolar broadening will occur at the same temperature as the $T_{1\rho}$ minimum. Importantly, the derivation of rates of molecular motions from relaxation time measurements is independent of whether there is a coalescence phenomenon possible or not. Thus, $T_{1\rho}$ measurements will provide activation data for rotations of both the phenyl and *tert*-butyl groups that display coalescence phenomena and for the isopropyl and *tert*-amyl groups that do not. The range of rates can equally be extended in the lower limit by magnetisation transfer or 2D CPEXSY measurements where rates comparable with ^{13}C relaxation times are accessible.[16,17] Using such methods we have measured rates as low as 10 s^{-1}. Thus, six orders of magnitude in rates of rotation are, in principle, available for study using these ^{13}C CP/MAS NMR techniques with almost continuous coverage of the range. The range may be extended further by use of T_1 and T_2 measurements.[3]

Some further points need to be made with regard to changes in $T_{1\rho}$ and with respect to $T_{1\rho}$ minima (see ref. 5 for a more detailed theory) since these are used extensively in this work. Cross polarised (CP) spectra require a transfer of polarisation from ^{1}H to ^{13}C which occurs at a given rate with time constants in the millisecond range. Whilst the polarisation is being transferred it is also being lost from both the ^{1}H and ^{13}C reservoirs by the $T_{1\rho}$ mechanism. Thus, efficient $T_{1\rho}$ relaxation leads to a reduction in signal intensity in CP spectra. To determine absolute rates from $T_{1\rho}$ data requires one to obtain the minimum value of $T_{1\rho}$ and to know the precessional frequency of the ^{13}C nuclei in the spin locking field (ω_1). $T_{1\rho}$ minima will be deeper for groups with strong dipolar interactions and for those that are close to the motion causing the relaxation. For example, a methyl rotation can cause extremely efficient $T_{1\rho}$ relaxation for the central carbon, whereas the central carbon in a *tert*-butyl group with no directly bound ^{1}H is less efficiently relaxed by this mechanism.

Because most of our earlier work in this area had involved *tert*-butyl groups we decided to extend our measurements to other groups and to attempt to measure the rotation rates of isopropyl and *tert*-amyl groups in a homologous series. The series chosen was compounds **6**–**10a,b,c**. The idea behind the design of this molecular series was to arrange for the molecules to contain molecular fragments that would not move and thus form a 'rigid and interlocking' reference frame against which the motions of the test groups could be studied. We chose a series of ammonium salts partly to ensure crystallinity but also for ease of synthesis and we chose to make benzyl ammonium salts in the view, naive as it turned out, that the benzyl groups would interact to form an interlocking rigid reference frame. Thus, the group rotations we were searching for were those of *N*-isopropyl, *N*-*tert*-butyl and *N*-*tert*-amyl.

At the outset we made several generalised predictions in accordance with our ideas about least distress. (i) The local C_{3v} symmetry of the *N*-*tert*-butyl groups should allow observations of *N*-*tert*-butyl rotations. (ii) The groups of lower local symmetry isopropyl (C_{2v}) and *tert*-amyl (at best C_{2v}) should show higher barriers. (iii) Since the proportional change in volume from methyl to hydrogen as an isopropyl group rotates is greater than from methyl to ethyl as a *tert*-amyl group rotates, rotations would be more likely to be observed for *tert*-amyl groups than for isopropyl groups.

Experimental

Preparation of compounds

Standard procedures were employed and are given below.

(A) Preparation of *N*-benzylalkylammonium bromides. Benzyl bromide (3.42 g 0.02 mol) was added to a large excess of amine (50 cm^3) slowly with cooling and the resultant precipitate was filtered off and recrystallised from ethanol/ether.

(B) Benzoylation of amines. The amine (0.2 mol) was dissolved in NaOH solution (240 cm^3, 5%) and to this was added benzoyl chloride (30 g, 0.21 mol). The mixture was stirred vigorously for 2 h and the resultant precipitate filtered off, recrystallised (ethanol) and dried to give white crystals.

(C) Alkylation of amides. NaH (4.4 g, 0.11 mol; 60% in oil) was dissolved in dry THF (100 cm^3) and to this was added the amide (0.1 mol) and the mixture was heated under reflux for 1 h. After this time the appropriate alkyl halide (0.11 mol) was added and the heating continued for a further 2 h. Water (80 cm^3) was added and the organic layer separated, dried (anhydrous $MgSO_4$) and the solvent removed to leave a crystalline solid which was recrystallised from ethanol.

(D) Reduction of amides. The amide (0.04 mol) was dissolved in dry THF (20 cm^3) and added dropwise to a solution of $LiAlH_4$ (1.48 g, 0.044 mol) in dry THF (50 cm^3). The mixture was heated under reflux for 1 h after which time NaOH (1.48 g, 0.04 mol) in water (1 cm^3) was added to give a granular white precipitate. The solvent was decanted, dried (anhydrous K_2CO_3) and the solvent removed to give the amine.

(E) Hydrobromination of the amine. The amine (0.01 mol) was dissolved in ethanol (20 cm^3) and to this was added 48% hydrobromic acid (1.69 g, 0.01 mol). The solvent was removed leaving a white solid which was recrystallised from ethanol/ether.

(F) Dimethylation of an amine (Eschweiller–Clark reaction). The amine (0.25 mol) was added to 40% aqueous formaldehyde (35 g, 0.5 mol) in water with cooling in ice/water. To this was added 98% formic acid (23.5 g, 0.5 mol) and the solution was then heated under reflux for 6 h. After this time NaOH pellets (10 g, 0.25 mol) were added. The resultant organic layer was separated, dried (anhydrous K_2CO_3) and distilled.

(G) Benzylation of dimethylamines. The amine (0.04 mol) was added to a solution of benzyl bromide (6.84 g, 0.04 mol) in ethanol (20 cm^3) and the mixture was heated under reflux for

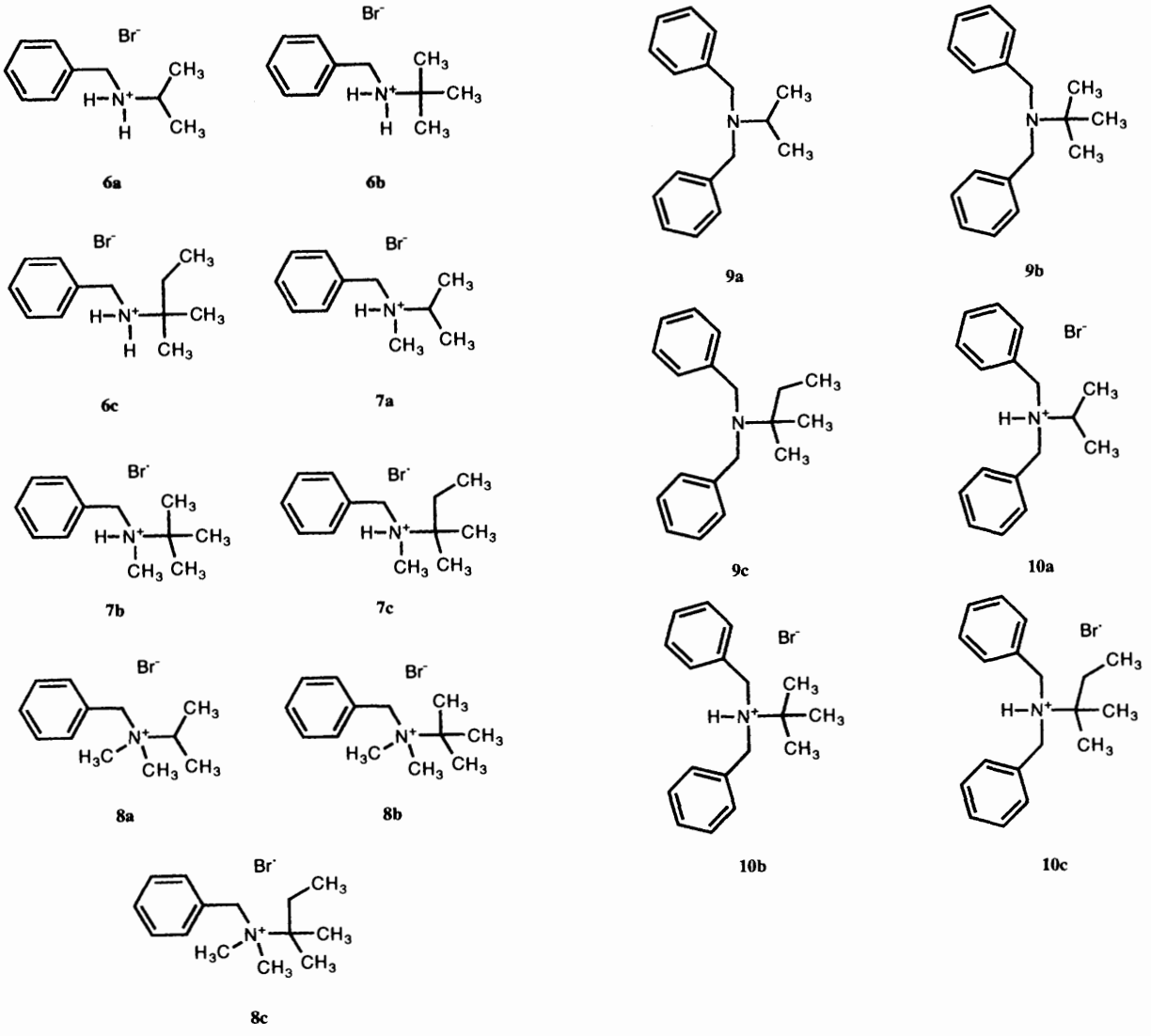

1 h. The solvent was removed leaving a white solid which was recrystallised from ethanol/ether.

(H) Preparation of *N*-benzyl- and *N*,*N*-dibenzylisopropylamine. Isopropylamine (11.8 g, 0.2 mol) was added to NaOH (8 g, 0.2 mol) in water and to this was added benzyl bromide (34.2 g, 0.2 mol) and the solution was stirred overnight. The organic layer which separated out was found to contain a mixture of amines and was then distilled to yield *N*-benzylisopropylamine (7.6 g, 51%) as a colourless oil. The residue from the distillation contained *N*,*N*-dibenzylisopropylamine which was purified by recrystallisation from ethanol (6.34 g, 27%).

Compounds **6a**,**b** and **c** were prepared by procedure A.

Compound **7a** was prepared by the sequence of procedures H, F, E.

Compounds **7b** and **c** were prepared by the sequence of procedures B, C, D and E.

Compounds **8a**,**b** and **c** were prepared by the sequence of procedures F and G.

Compound **9a** was prepared by procedure H.

Compounds **9b** and **c** were prepared by the sequence of procedures B, C and D.

Compounds **10a**,**b** and **c** were prepared by the sequence of procedures B, C, D and E.

All products and intermediates had solution state NMR spectral data in accord with their structures. Data on which characterisations of the products were made and their mps are given in Table 1. Details of the physical characteristics of intermediates are presented in ref. 19.

NMR spectra

Solid state ^{13}C CP/MAS NMR spectra were obtained on a Bruker MSL 500 spectrometer at 125.758 MHz using 4 mm o.d. zirconia rotors. The following typical conditions were employed: contact time 1 ms, spectral width 30 000 Hz, acquisition time 17.4 ms, spin locking field frequency *ca.* 60 kHz, recycle delay 5 s, spinning speeds 6–8 kHz. Chemical shifts were referenced to the CH_2 resonance in an external adamantane sample at 38.56 ppm. Dipolar dephased [Non Quaternary Suppressed (NQS)] spectra were obtained by a standard sequence incorporating a 50 μs dipolar dephasing delay. $T_{1\rho}$ measurements were performed as described previously using a standard $T_{1\rho}$ sequence preceded by cross polarisation. Spin lock periods of up to 20 ms were employed with ^{13}C precessional frequencies (ω_1) of *ca.* 60 kHz. Temperatures in the MAS probe were calibrated as described previously [5] using standard samples with known phase changes run under conditions as close to those of the experimental observations as possible. Separate experiments show that with the current stator block design employed in the spectrometer there is little temperature variation with spinning rate at the rates employed here. 2D CP EXSY spectra were determined using a standard 2D EXSY pulse sequence in which a cross polarisation sequence replaces the first 90° pulse.

Line shape analyses for a three site system were calculated using a computer program kindly supplied by Dr J. E. Anderson. Matching of calculated and observed spectra was done by visual comparison, by measurements of relative heights of peaks and valleys and by measurements of line widths.

Table 1 Elemental analyses and melting points for the synthesised compounds

Compound	Formula	Mp (°C)	Carbon		Hydrogen		Nitrogen	
			Required	Found	Required	Found	Required	Found
6a	$C_{10}H_{16}NBr$	215–216	52.19	52.09	7.01	7.06	6.09	6.34
b	$C_{11}H_{18}NBr$	236–238	54.11	54.38	7.43	7.24	5.74	5.45
c	$C_{12}H_{20}NBr$	207–208	55.82	55.76	7.81	7.41	5.42	5.68
7a	$C_{11}H_{18}NBr$	132–134	54.11	54.10	7.43	7.50	5.74	5.93
b	$C_{12}H_{20}NBr$	180–181	55.82	55.68	7.81	8.15	5.42	5.47
c	$C_{13}H_{22}NBr$	156–157	57.36	57.36	8.15	8.41	5.15	5.26
8a	$C_{12}H_{20}NBr$	205–206	55.82	56.01	7.81	7.94	5.42	5.42
b	$C_{13}H_{22}NBr$	196–197	57.36	57.75	8.15	7.78	5.15	5.10
c	$C_{14}H_{24}NBr$	174–175	58.74	59.14	8.82	9.16	4.89	4.96
9a	$C_{17}H_{21}N$	33–34	85.31	85.51	8.84	9.03	5.85	5.85
b	$C_{18}H_{23}N$	66–68			Lit. mp 68–70 °C (ref. 18)			
c	$C_{19}H_{25}N$	41–42	85.32	85.73	9.42	9.84	5.24	5.26
10a	$C_{17}H_{22}NBr$	162–163	63.75	63.75	6.92	6.91	4.37	4.37
b	$C_{18}H_{24}NBr$	190–191	64.67	64.91	7.24	7.29	4.19	4.17
c	$C_{19}H_{26}NBr$	207–208	65.52	65.94	7.52	7.87	4.02	4.04

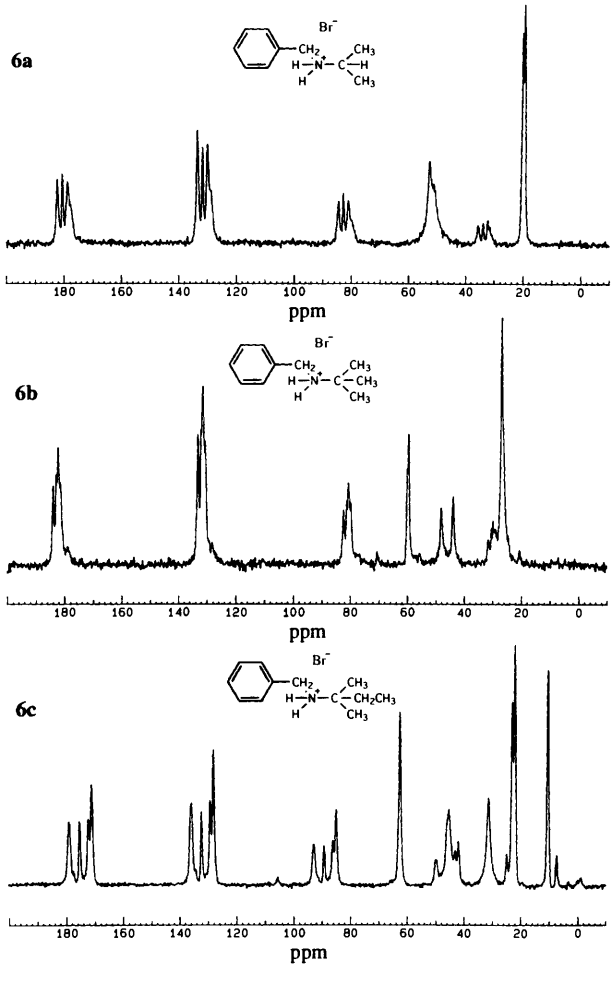

Fig.1 Room temperature ^{13}C CP/MAS NMR spectra of compounds **6a–c** at 125.758 MHz

Solution state ^1H and ^{13}C NMR spectra were obtained from $CDCl_3$ or D_2O solutions in a 5 mm tube using the high resolution probe in the MSL 500 spectrometer or on either a Bruker AM 300 or a Varian Gemini 200 spectrometer.

Activation parameters were derived from Eyring or Arrhenius plots of the rate data or from plots of $\ln(T_{1\rho})$ *vs.* T^{-1}. The theory and details of these methods are discussed in refs. 5 and 7. Errors on the activation parameters quoted in this paper are 95% confidence limits estimated as twice the standard deviation calculated from least-squares linear plots. Errors on the $T_{1\rho}$ values in this paper vary with the signal to noise ratio available from the sample in a reasonable time period. They would typically be around ± 5%.

Details of the X-ray powder diffraction structure determination are given in ref. 8.

Results and discussion

All CP/MAS NMR spectra display spinning side bands displaced from the original resonance by the spinning frequency unless this is larger than the chemical shift anisotropy. In all the spectra in this paper no spinning side-bands were observed for the aliphatic or benzylic resonances but appreciable spinning sidebands were observed for the aromatic resonances. The aromatic signals occur between 120 and 140 ppm. Their spinning sidebands are symmetrically displaced from them and second-order spinning sidebands are sometimes visible in the aliphatic region. The sidebands never interfered with the observations of dynamic phenomena.

The room temperature ^{13}C CP/MAS spectra of compounds **6a–c** are shown in Fig. 1. The spectrum of **6a** is consistent with one molecule in the asymmetric unit of the crystal and unless otherwise stated this is true for all other compounds studied. The isopropyl methyls are at 19 and 20 ppm, the benzylic CH_2 and the *N*-CH overlap at 53 ppm and the aromatic ring carbons are at *ca.* 130 ppm. Variable temperature spectra show no variations in the patterns for the aliphatic portions of the molecule. However, at low temperatures the aromatic region consists of four lines with two of relative intensity two. On warming there is an apparent coalescence of two lines at 128 and 129.5 ppm followed *ca.* 50 K higher in temperature by a loss in signal intensity of all but two lines, those at 129.5 and 131.5 ppm (Fig. 2). Such behaviour is consistent with other examples we have seen of phenyl rotations.[7,8] The lower temperature coalescence is followed at higher temperatures by loss of signal intensity due to a reduction in $T_{1\rho}$ accompanied by dynamic line broadening. The two lines unaffected throughout the temperature range are from the carbon atoms along the axis of rotation. No attempt was made to determine the temperature variation of rates in this compound. We note, however, that the apparent doublet coalescence at 293 K gives an approximate free energy of activation for the phenyl ring rotation process of *ca.* 55 kJ mol^{-1}.

The spectrum of **6b** shows that there are two independent molecules in the asymmetric unit (designated **6bi** and **6bii**). We have previously shown that the same molecule in two different solid phases shows different activation parameters for *tert*-butyl group rotation. This compound forms a test as to whether two independent but otherwise identical molecules in the

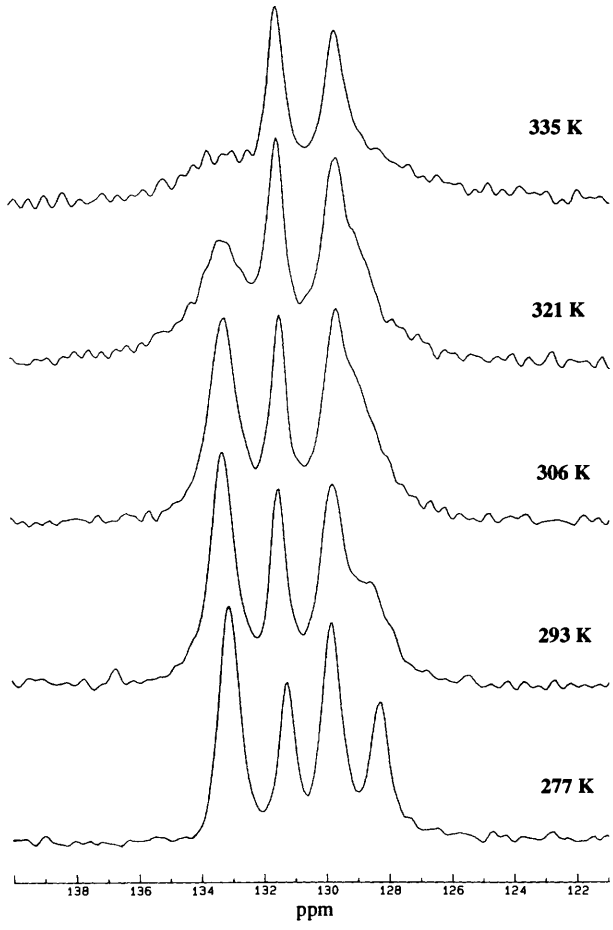

Fig. 2 Temperature variation of the ^{13}C CP/MAS NMR spectrum of the aromatic region of compound **6a** at 125.758 MHz

Table 2 $T_{1\rho}$ (ms) and rate (s^{-1}) data for compound **6b**; [ω_1 = 61 kHz][a]

43 ppm (**6bii**)			47 ppm (**6bi**)		
T/K	$T_{1\rho}$	k	T/K	$T_{1\rho}$	k
371	25.95	1.2×10^6	255	54.34	1.0×10^7
364	19.69	6.4×10^5	248	34.06	6.1×10^6
357	20.86	8.1×10^5	240	39.68	7.2×10^6
342	19.93	4.6×10^5	233	17.64	1.5×10^6
335	19.76	4.8×10^5	226	20.88	9.1×10^5
321	25.36	2.6×10^5	219	20.84	9.2×10^5
313	28.17	2.2×10^5	212	20.43	6.4×10^5
306	39.93	1.5×10^5	205	28.16	5.9×10^5
Line shape data					
270		2.5×10^4			
263		1.0×10^4			
255		4.0×10^3			

[a] Rates from line shape data derived by line fitting. Rates from $T_{1\rho}$ data determined as in ref. 5.

asymmetric unit show different activation parameters for *tert*-butyl group rotation. In the high temperature region the methyls in both *tert*-butyl groups give overlapping resonances at 27 ppm with the quaternary carbon resonances overlapping at 60 ppm. However, the benzyl CH_2 units are widely separated at 43 and 47 ppm and the aromatic carbons are at *ca.* 130 ppm with the dipolar dephased (NQS) spectrum showing two quaternary aromatic carbons. Because the *tert*-butyl methyl lines are relatively sharp singlets the *tert*-butyl groups are rotating rapidly at room temperature. The overlap precluded the measurement of $T_{1\rho}$ values from the methyl carbons; however, two other carbons are available to provide such information, the benzylic CH_2 units. Although these are more

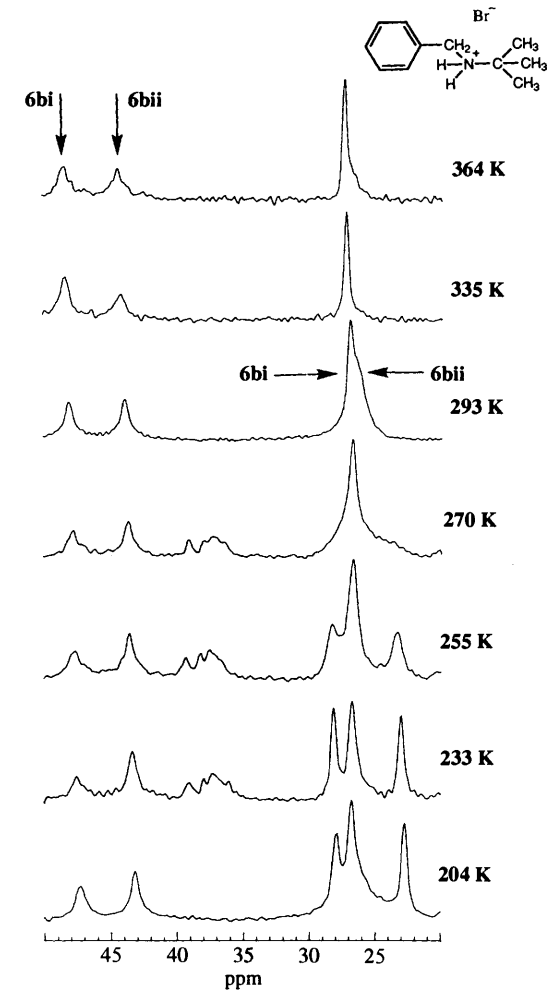

Fig. 3 Representative ^{13}C CP/MAS NMR spectra of **6b** at 125.758 MHz showing the *tert*-butyl coalescences and the variation in intensity of the N–CH_2 resonances

remote sensing groups for the *tert*-butyl rotation they are adjacent to the *tert*-butyl group and should, therefore, report the same information.

Representative spectra over the temperature range 204–364 K are shown in Fig. 3 and $T_{1\rho}$ values and derived rate constants are given in Table 2. The $T_{1\rho}$ data on the CH_2 carbon resonances for the two independent molecules show minima that are *ca.* 100 K apart, with the resonance at 43 ppm belonging to the slower rotating molecule **6bii**. The $T_{1\rho}$ minimum for **6bii** occurs at 335 K and the signal from the *tert*-butyl methyls has essentially vanished at this temperature leaving the methyl spectrum for **6bi**. When this spectrum was subtracted from those at lower temperatures an approximation to the line shape changes for the methyl groups in **6bii** was obtained. Calculation of rates from these spectra gave the data shown in the lower portion of Table 2. The rates fall close to the activation plot derived from the CH_2 $T_{1\rho}$ data giving confidence in the validity of the rates derived from the $T_{1\rho}$ data. The Arrhenius activation plots give very different energies of activation (**6bi** *ca.* 43.1, **6bii** *ca.* 26.7 kJ mol^{-1}). As expected, the $T_{1\rho}$ minima are higher than those observed for *tert*-butyl groups in other compounds but have almost identical relaxation time minima as would be expected for similar molecular motions.

Enthalpies and entropies of activation of low reliability can be calculated from the rate data and suggest that the principal effect governing the differences in rate is the entropy of activation. Comparable rates for the *tert*-butyl rotation in the two independent molecules are *ca.* 150 K apart with **6bii** having the slower rates. Alternatively put, at ambient temperature (293 K), a temperature partway between the two experimental

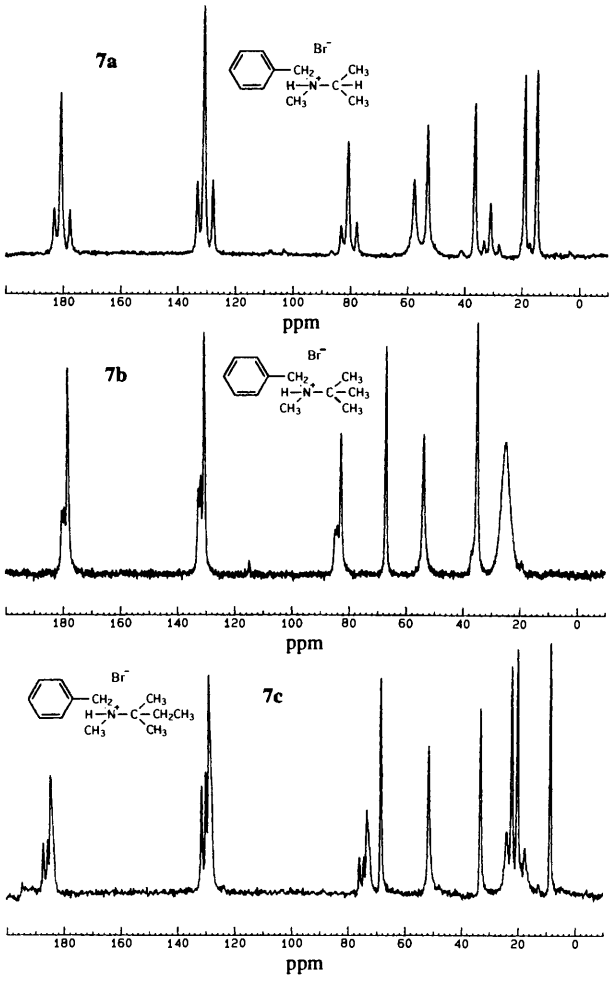

Fig. 4 Room temperature ^{13}C CP/MAS NMR spectra of compounds **7a–c** at 125.758 MHz

Table 3 $T_1\rho$ (ms) and rate (s^{-1}) data for compound **7b**; [ω = 61 kHz][a]

	25 ppm		67 ppm	
T/K	$T_{1\rho}$	*k*	$T_{1\rho}$	*k*
371	4.67	6.4×10^6	6.21	1.4×10^6
364	4.46	3.8×10^6	6.14	1.2×10^6
357	3.21	2.0×10^6	7.63	5.8×10^5
350	2.76	1.0×10^6	7.35	6.2×10^5
342	4.79	3.7×10^5	11.14	3.5×10^5
335	6.21	2.7×10^5	16.26	2.3×10^5
328	8.48	1.9×10^5	23.69	1.5×10^5
320	12.32	1.3×10^5	39.20	9.0×10^4
Line shape data				
293		3.5×10^4		
283		1.5×10^4		
280		8.0×10^3		
277		4.5×10^3		

[a] Rates from line shape data derived by line fitting. Rates from $T_{1\rho}$ data determined as in ref. 5.

temperature ranges, the free energies of activation ($\Delta G^{\ddagger}$) calculated from the derived enthalpies and entropies of activation are calculated to be 40.9 kJ mol^{-1} **6bi** and 28.7 kJ mol^{-1} **6bii**. These free energies of activation are similar to the activation energies discussed above. This is an interesting example of two otherwise identical molecules occupying different positions in the asymmetric unit of the solid having different rates and activation parameters for a solid state conformational process. A related phenomenon involving two independent phenyl rings in the same molecule has been observed.[20]

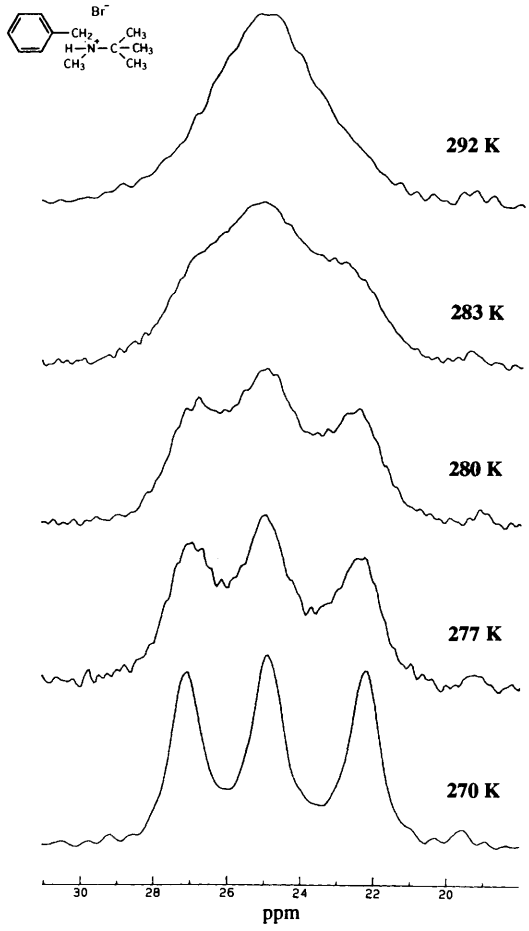

Fig. 5 Temperature variation of the ^{13}C CP/MAS NMR spectrum of the *tert*-butyl region of compound **7b** at 125.758 MHz

The spectrum of **6c** shows the carbons in the *tert*-amyl group as follows: methyls at 22 and 23 ppm, ethyl CH_2 at 31 and methyl at 10 ppm and the central carbon at 62 ppm. The benzylic CH_2 is at 45 ppm and the aromatic carbons are at *ca.* 130 ppm. No changes were observed in the variable temperature spectra of this compound and we conclude that the rates of any molecular motions are in regions outwith the detection limits of our techniques.

The room temperature ^{13}C CP/MAS spectra of compounds **7a–c** are shown in Fig. 4. The spectrum of **7a** shows the isopropyl methyls at 15 and 19 ppm. The *N*-CH and *N*-CH_3 are at 58 and 37 ppm, respectively. The benzylic CH_2 is at 53 ppm and the aromatic carbons are at *ca.* 130 ppm. No effects attributable to dynamic processes are observed in the ^{13}C CP/MAS spectra as the temperature is varied.

The spectrum of **7b** has a broad signal at 25 ppm due to the *tert*-butyl methyls. The signal is dynamically broadened due to the rotation of the *tert*-butyl group. The central *tert*-butyl carbon and the *N*-methyl are at 67 and 35 ppm, respectively. The benzylic CH_2 is at 54 ppm with the aromatic carbons at *ca.* 130 ppm. On cooling from ambient temperature the *tert*-butyl methyl signal broadens further and splits into a triplet (Fig. 5). On warming above room temperature this signal sharpens and then undergoes a reduction in relative intensity as $T_{1\rho}$ relaxation becomes more rapid and then starts to recover its relative intensity at even higher temperatures. Table 3 records the $T_{1\rho}$ and rate data for this compound. The combination of rates determined from the $T_{1\rho}$ measurements and the line shape changes give the following activation parameters for *tert*-butyl rotation: $\Delta H^{\ddagger}$ = 54.9 ± 7.8 kJ mol^{-1} and $\Delta S^{\ddagger}$ = 17.8 ± 22.9 J K^{-1} mol^{-1}.

The spectrum of **7c** shows the carbons in the *tert*-amyl group as follows: methyls at 22 and 24 ppm, ethyl CH_2 at 26 and

Table 4 $T_{1\rho}$ (ms) and rate (s^{-1}) data for compound **7c**; [ω_1 = 62 kHz][a]

	11 ppm		22 ppm		24 ppm		68 ppm	
T/K	$T_{1\rho}$	k	$T_{1\rho}$	k	$T_{1\rho}$	k	$T_{1\rho}$	k
371	8.53	3.2×10^6	4.13	1.2×10^6	4.27	2.1×10^6	9.4	2.9×10^6
364	5.47	1.2×10^6	4.45	8.2×10^5	3.67	1.2×10^6	6.5	1.2×10^6
357	8.37	4.4×10^5	6.13	4.6×10^5	5.85	4.1×10^5	12.2	3.4×10^5
349	12.43	2.7×10^5	9.27	2.7×10^5	9.03	2.5×10^5	21.4	1.8×10^5
342	20.64	1.6×10^5	13.3	1.9×10^5	12.6	1.8×10^5	37.2	1.0×10^5
335	31.79	1.0×10^5	18.2	1.3×10^5	16.7	1.3×10^5	53.3	7.2×10^4
327	46.64	6.9×10^4	29.1	8.3×10^4	21.1	1.1×10^5		
320			39.6	6.2×10^4	31.7	6.8×10^4		
313			46.2	5.2×10^4	40.8	5.3×10^4		

[a] Rates from $T_{1\rho}$ data determined as in ref. 5.

Table 5 $T_{1\rho}$ data (ms) for compound **8a**

51 ppm	
T/K	$T_{1\rho}$
262	8.45
255	6.69
247	4.68
240	3.07
232	2.24
225	1.05

methyl at 11 ppm and the central carbon at 68 ppm. The *N*-methyl is at 35 ppm with the benzylic CH_2 at 53 ppm and the aromatic carbons are at *ca.* 130 ppm. On warming there is a loss in relative intensity of the *tert*-amyl resonances. This loss in relative intensity is associated with reductions in $T_{1\rho}$ which are recorded in Table 4. Minima in the $T_{1\rho}$ values are observed in the region around 360–370 K. The only reasonable explanation for the behaviour of the $T_{1\rho}$ values which are similar to those we have previously observed for *tert*-butyl groups is that it originates from a *tert*-amyl group rotation. In this case there can, however, be no coalescence data to confirm this conclusion because the *tert*-amyl methyl groups are diastereotopic (even in the free molecule) and therefore have different chemical shifts whatever the rate of rotation. The alternative explanation that the observations could arise from rotation of the ethyl group in the *tert*-amyl is unreasonable in view of the very low $T_{1\rho}$ minimum (Table 4) observed for the *tert*-amyl methyls. This low value means that they are participants in the motion and not spectators. (See compound **6b** above for an analogy.) Finally, the possibility that the results could arise from a disordered crystal can be discounted. The ambient temperature spectrum is clearly that of a single crystalline form displaying sharp lines and the spectrum shows none of the multiplicity that would be expected from a disordered crystal (the small peak at *ca.* 18 ppm is a spinning side band on the phenyl resonances).

The rates derived from the $T_{1\rho}$ values for all four carbons differ most at the upper end of the temperature range by a factor of about 2.5. The rates for the two methyl groups at 22 and 24 ppm, however, are reasonably consistent throughout the temperature range. The Arrhenius plot of ln(*k*) *vs.* T^{-1} is, however, curved and not linear as we have observed in all other cases. It may be that the reason this *tert*-amyl group is relatively free to rotate is that its ethyl group is rotating relatively freely too. If this is the case the ethyl group can 'get out of the way' as the *tert*-amyl group rotates. Since we expect each carbon to report principally on its own motion, this type of behaviour should show rates for the two *C*-methyls that are similar, but rates for the methyl and the ethyl group that are different and we should get curved Arrhenius plots, as is observed. From the Arrhenius plot for the rates for the two *C*-methyls an approximate energy of activation of 58 kJ mol^{-1} is obtained. We believe that this report is the first published example of the measurement of the rate of rotation of a *tert*-amyl group in a solid.

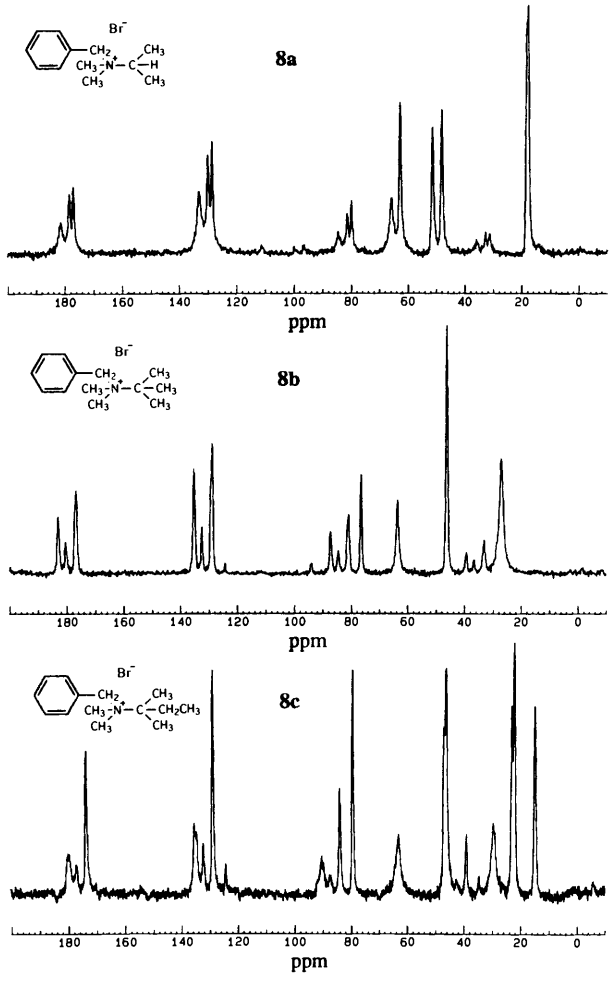

Fig. 6 Room temperature ^{13}C CP/MAS NMR spectra of compounds **8a–c** at 125.758 MHz

The room temperature ^{13}C CP/MAS spectra of compounds **8a–c** are shown in Fig. 6. The spectrum of compound **8a** shows the two isopropyl methyls overlapping at 18 ppm. The *N*-CH and the two *N*-methyls are located at 66, 51 and 48 ppm, respectively. The benzylic CH_2 is at 63 ppm and the aromatic carbons are at *ca.* 130 ppm. Variable temperature studies show no significant changes in the resonances of the isopropyl carbons. However, as the temperature is lowered the peak from one of the *N*-methyls (51 ppm) broadens and reduces in intensity until by 208 K it is no longer visible. The other *N*-methyl peak is unaffected. If the spectra are obtained using single carbon pulses and high power decoupling the 51 ppm

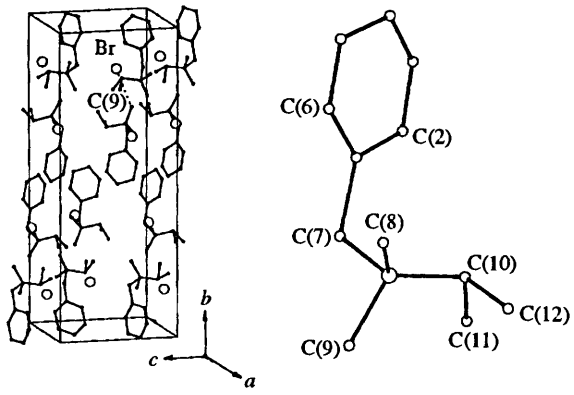

Fig. 7 Molecular structure and structure of the unit cell of **8a** determined by powder X-ray diffraction.[6]

peak is still visible but broadened at 208 K. Measurements of $T_{1\rho}$ for the 51 ppm methyl peak (Table 5) confirm that its disappearance is due to a reduction in its $T_{1\rho}$ value which falls to less than 0.5 ms by 208 K. Because a minimum in the $T_{1\rho}$ *vs.* temperature curve could not be determined a plot of $\ln(T_{1\rho})$ *vs.* T^{-1} was performed in order to obtain the activation energy for the methyl group rotation which was found to be 26.6 ± 4.2 kJ mol^{-1}.[6]

The structure of **8a** was determined by powder X-ray diffraction (Fig. 7).[8] The structure shows two features that are particularly significant in rationalising the NMR data of the *N*-methyl group discussed above. First, the C9 methyl group has a dihedral angle of 43° along the N–C bond to one of the isopropyl methyl groups. This is significantly smaller than the ideal value of 60°. Secondly, the C9 atom is also significantly closer to the Br^- ion than any other carbon atom, having near neighbour Br^- ions at 368 and 385 pm. The corresponding closest contacts for the other *N*-methyl carbon, C8, are 392 and 394 pm. The extent of the pressure exerted by the bromide upon the C9 methyl is illustrated by the fact that the C9 to bromide vector is in the correct direction to reduce the dihedral angle between C9 and its isopropyl neighbour from the ideal value of 60° to the observed value of 43°. Hence the powder diffraction data clearly show that one of the methyl groups, C9, is substantially more hindered than the other.

At low temperatures five aromatic carbon resonances can be distinguished in the spectrum with that at 133 ppm being of relative intensity 2 (Fig. 8). As the temperature is raised coalescences are observed at *ca.* 280 K involving the resonances at 127, 131.5 and 133 ppm. At higher temperatures still (*ca.* 310 K) loss of signal intensity and dynamic line broadening are observed. These observations are consistent with a phenyl group rotation taking place in the solid. No attempt was made to obtain rate data or activation parameters but the observations suggest rates in the region 3 × 10^2 s^{-1} at 280 K ($\Delta G^{\ddagger}_{280}$ = *ca.* 50 kJ mol^{-1}) and 5 × 10^4 s^{-1} at 335 K ($\Delta G^{\ddagger}_{335}$ = *ca.* 52 kJ mol^{-1}).

The crystal structure (Fig. 7)[8] again is of use in explaining the observations on the phenyl rotation showing that the phenyl rings are relatively unencumbered. The closest approach of carbon atoms between the phenyl rings in adjacent molecules is 396 pm. One adjacent ring is parallel and the other adjacent ring is at an angle of approximately 65°. There is appreciable space in which the phenyl groups may rotate.

The spectrum of **8b** shows the *tert*-butyl methyl resonance as a single broad line at 27 ppm with the quaternary carbon at 76 ppm. The two *N*-methyls are superimposed at 46 ppm. The benzylic CH_2 is at 64 ppm with the aromatic carbons at *ca.* 130 ppm. As the sample is cooled the *tert*-butyl methyl resonance splits into a 1:1 doublet (Fig. 9). This unexpected behaviour suggests that one of the methyl resonances is missing or extremely broad. Plots of chemical shift above and below coalesence confirm that there is a resonance missing which

Table 6 $T_{1\rho}$ (ms) and rate (s^{-1}) data for compound **8b**; [ω_1 = 61 kHz][a]

27 ppm		
T/K	$T_{1\rho}$	*k*
349	3.74	5.2 × 10^6
342	5.25	7.8 × 10^6
335	2.34	2.1 × 10^6
327	2.74	3.3 × 10^6
320	2.23	1.8 × 10^6
312	3.06	8.1 × 10^5
305	3.78	6.1 × 10^5
298	3.53	6.7 × 10^5
290	4.74	4.6 × 10^5
283	6.88	3.5 × 10^5
224		3.3 × 10^2

[a] Rates from $T_{1\rho}$ data determined as in ref. 5.

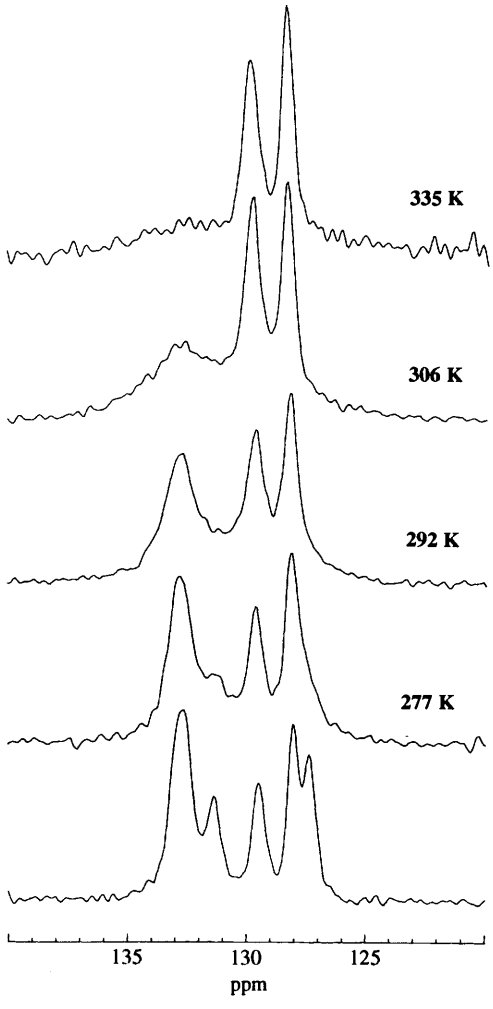

Fig. 8 Temperature variation of the ^{13}C CP/MAS NMR spectrum of the aromatic region of compound **8a** at 125.758 MHz

should be at *ca.* 25 ppm below the coalescence temperature. In fact, there is an asymmetry in the spectrum obtained at 210 K which is consistent with this observation. We conclude that one of the methyls is substantially more hindered than the others and that there is a slowing of a methyl rotation taking place as well. This leads to a reduction in $T_{1\rho}$ with reduced cross polarisation efficiency and associated dynamic line broadening.

At higher temperatures the *tert*-butyl methyls exhibit a reduction in $T_{1\rho}$ associated with the rate of rotation of the *tert*-butyl group being similar to the precessional frequency of the ^{13}C nuclei in the spin lock field. These measurements are given in Table 6 in which the rate given at 224 K is obtained from the

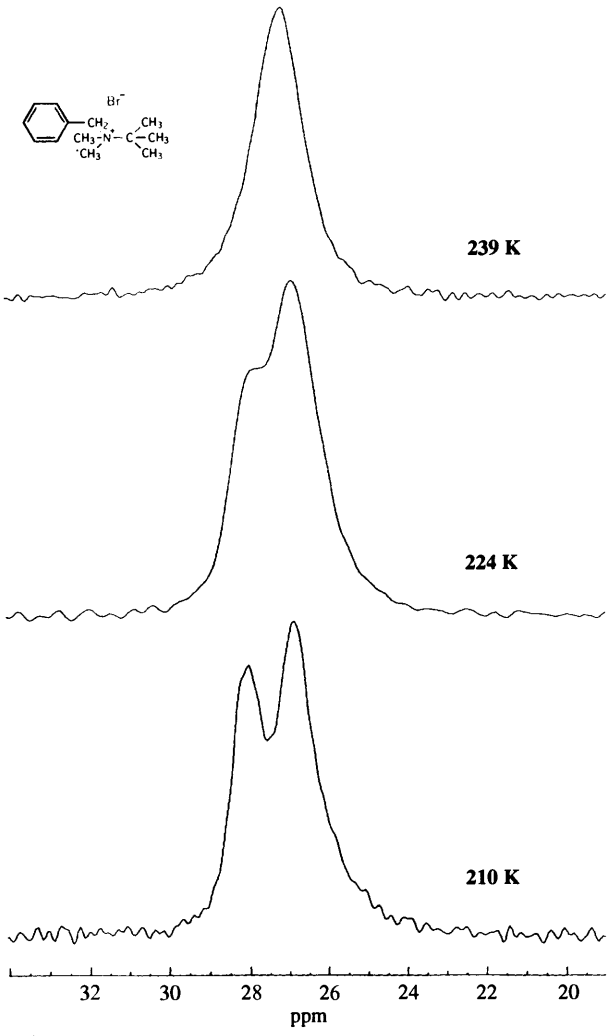

Fig. 9 Temperature variation of the ^{13}C CP/MAS NMR spectrum of the *tert*-butyl region of compound **8b** at 125.758 MHz

Table 7 $T_{1\rho}$ (ms) and rate (s^{-1} data for compound **9b**; [ω_1 = 60 kHz][a]

	27 ppm	
T/K	$T_{1\rho}$	*k*
290	19.23	3.2×10^7
283	11.73	1.9×10^7
276	8.43	1.4×10^7
268	4.76	7.4×10^6
265	4.61	7.1×10^6
261	3.98	6.0×10^6
257	3.85	5.8×10^6
253	2.92	3.9×10^6
250	2.97	4.1×10^6
246	2.24	1.8×10^6
243	2.31	1.4×10^6
238	2.43	1.2×10
232	3.37	7.0×10^5
224	3.09	7.9×10^5
217	3.41	6.9×10^5

[a] Rates from $T_{1\rho}$ data determined as in ref. 5.

coalescence point. The use of $T_{1\rho}$ data to obtain rates of rotation of *tert*-butyl groups requires that the rates of rotation of the individual methyl groups are considerably faster than the rate of rotation of the *tert*-butyl group. Therefore, the derived rates and activation parameters for this compound must be regarded with caution.

The spectrum of compound **8c** shows the *tert*-amyl methyls at 22 and 23 ppm and the quaternary carbon at 80 ppm. The ethyl

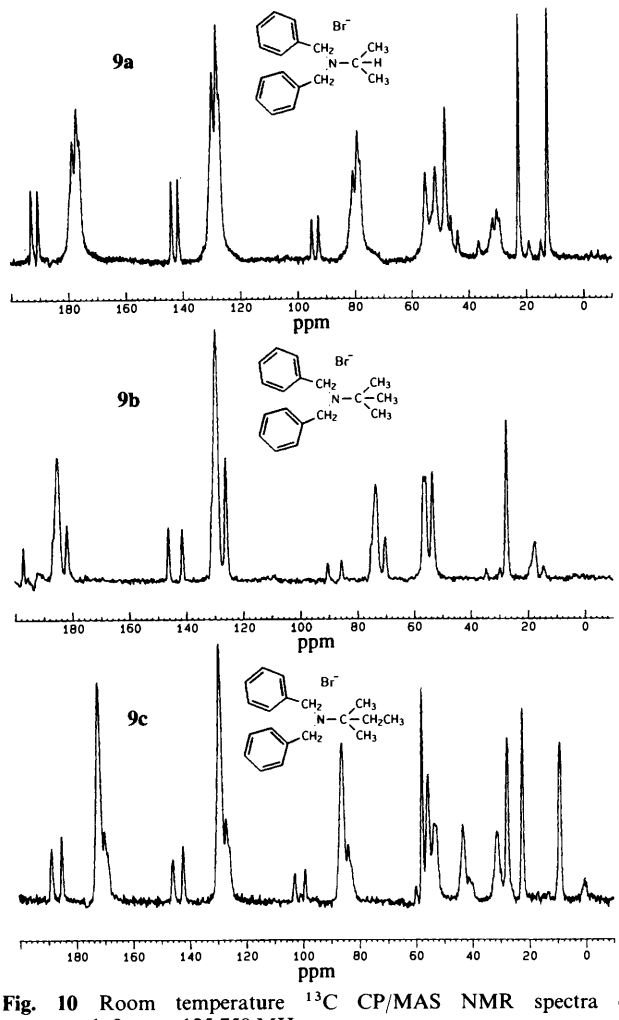

Fig. 10 Room temperature ^{13}C CP/MAS NMR spectra of compounds **9a–c** at 125.758 MHz

CH_2 and methyl are located at 29 and 15 ppm, respectively. The *N*-methyls are at 46 and 47 ppm. The benzylic CH_2 is shown at 63 ppm with the aromatics *ca.* 130 ppm. Variable temperature spectra show no change in the relative intensity of the peaks. Any intramolecular motions occurring in this compound must be outside the measurable range of our techniques.

The quaternary ammonium salts investigated in this paper were all prepared from an appropriate amine precursor. The only series of these amines to be solids was the dibenzyl series **9a–c**. The room temperature ^{13}C CP/MAS spectra of this series are shown in Fig. 10. The spectrum of **9a** shows the isopropyl methyls at 13 and 23 ppm with the *N*-CH at 48 ppm. The benzylic CH_2 groups are at 52 and 55 ppm with the aromatic resonances at *ca.* 130 ppm. No changes were observed in the variable temperature spectra of this compound and we conclude that the rates of any molecular motions are in regions outwith the detection limits of our techniques.

The spectrum of **9b** shows the *tert*-butyl methyls as a broadened singlet of reduced relative intensity at 27 ppm. The central carbon is at 56 ppm and the benzylic CH_2 carbons are at 56 and 53 ppm. The aromatic carbons are at *ca.* 130 ppm. As the temperature is varied the *tert*-butyl resonances show dynamic effects (Fig. 11). On cooling to 184 K the *tert*-butyl methyl resonance splits into a 1:1 doublet. As with **8b** a plot of chemical shift *versus* temperature shows that one peak at *ca.* 30 ppm is missing at low temperature. The missing methyl is presumed to have a rate of rotation sufficiently slow to cause rapid $T_{1\rho}$ relaxation and dynamic line broadening. Measurements of the methyl $T_{1\rho}$ values above 217 K show behaviour consistent with *tert*-butyl rotation and the data with derived rate constants is shown in Table 7. Again in this case the rate

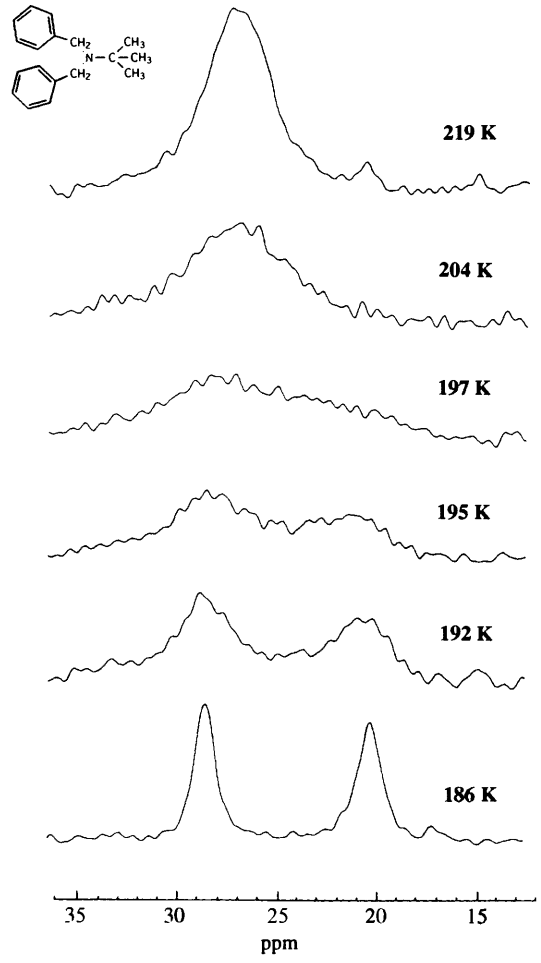

Fig. 11 Temperature variation of the ^{13}C CP/MAS NMR spectrum of the *tert*-butyl region of compound **9b** at 125.758 MHz

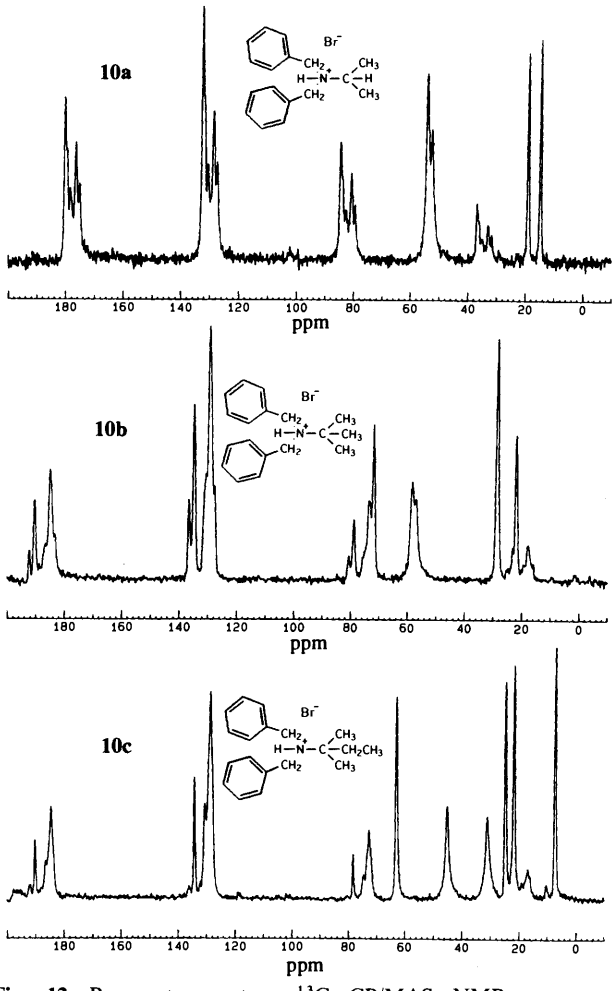

Fig. 12 Room temperature ^{13}C CP/MAS NMR spectra of compounds **10a–c** at 125.758 MHz

constants and derived activation parameters should be treated with caution because of the possibility that one of the methyls may not be rotating very much faster than the *tert*-butyl group.

The spectrum of compound **9c** shows the *tert*-amyl methyl carbons at 22 and 28 ppm with the ethyl CH_2 and methyl peaks at 32 and 9 ppm, respectively. The quaternary carbon is located at 58 ppm. The benzylic CH_2 carbons are at 54 and 56 ppm with the aromatic carbons at *ca.* 130 ppm. Variable temperature spectra show no changes attributable to dynamic processes which are therefore outwith the range measurable by our techniques.

The room temperature ^{13}C CP/MAS spectra of **10–c** are shown in Fig. 12. The spectrum of **10a** shows the isopropyl methyl carbons at 15 and 19 ppm with the *N*–CH at 54 ppm. The benzylic CH_2 carbons are at 52 and 54 ppm with the aromatic carbons at *ca.* 130 ppm. Variable temperature spectra show no changes attributable to dynamic processes which are therefore outwith the range measurable by our techniques.

The spectrum of **10b** shows the *tert*-butyl methyls already 'frozen out' at room temperature in a 2:1 ratio. The peaks broaden and start to coalesce on heating the sample (Fig. 13). The region in which $T_{1\rho}$ relaxation would be rapid for this compound is above the upper temperature limit for the probe so no measurements were attempted. Below coalescence, however, 2D CPEXSY experiments were performed to obtain rotation rates. These are recorded in Table 8.

The spectrum of **10** shows the *tert*-amyl methyl carbons at 22 and 25 ppm, the quaternary carbon at 63 ppm with the ethyl CH_2 and methyl at 31 and 7 ppm, respectively. The benzylic CH_2 carbons overlap at 45 ppm and the aromatic carbons are at *ca.* 130 ppm. Variable temperature spectra show no changes attributable to dynamic processes which are therefore outwith the range measurable by our techniques.

Table 8 2D CPEXSY rate data (s^{-1}) for compound **10b**

Methyls	
T/K	*k*
349	2.0×10^3
342	1.0×10^3
327	5.1×10^2
312	1.3×10^2
298	4.0×10^1
290	2.2×10^1
283	8.9×10^0

This work has reemphasised the validity and utility of CP/MAS methods for examining molecular dynamics in solids and has provided evidence of a remarkable variety of solid state conformational motions in a simple series of compounds. Motions that have been detected include rotations of methyl, *tert*-butyl, *tert*-amyl and phenyl groups. There may also be evidence of an ethyl group rotating inside a *tert*-amyl group. There is clearly much more conformational activity in solids than had previously been widely believed to be the case.

The combined activation parameters, where these have been determined, are given in Table 9. The activation parameters show a tremendous variation for same molecular motion in different compounds emphasising that conformational activation parameters in solids are determined by both inter- and intramolecular forces. The most reliable parameters are the energies of activation (E_a) and free energies of activation

Table 9 Activation parameters for group rotations[a]

Compound	Rotation type	E_a/ kJ mol^{-1}	$\Delta H^{\ddagger}$/ kJ mol^{-1}	$\Delta S^{\ddagger}$/ J K^{-1} mol^{-1}	$\Delta G^{\ddagger}_{293K}$/ kJ mol^{-1}
6a	phenyl				*ca.* 55
6bi	*tert*-butyl	*ca.* 43.1	24.2 ± 3.3	−57.3 ± 9.9	41.0 ± 6.2
6bii	*tert*-butyl	*ca.* 26.7	25.3 ± 8.7	−11.7 ± 38.3	28.7 ± 19.9
7b	*tert*-butyl		55.5 ± 5.7	27.9 ± 16.6	47.3 ± 10.6
7c	*tert*-amyl		54.9 ± 7.8	17.8 ± 22.9	49.7 ± 14.5
8a	phenyl				*ca.* 51
8a	methyl	26.6 ± 4.2			
8b	*tert*-butyl		47.7 ± 6.1	23.5 ± 20.3	40.8 ± 12.3
9b	*tert*-butyl		33.3 ± 3.1	13.32 ± 12.1	29.4 ± 6.6
10b	*tert*-butyl		59.4 ± 5.2	−33.9 ± 16.4	69.3 ± 10.0

[a] These data are obtained by either Arrhenius (E_a) or Eyring ($\Delta H^{\ddagger}$ and $\Delta S^{\ddagger}$) plots of the rate data obtained in Tables 2–8 or from plots of $\ln(T_{1\rho})$ *vs.* $1/T$ (E_a). $\Delta G^{\ddagger}_{293K}$ values are calculated from the $\Delta H^{\ddagger}$ and $\Delta S^{\ddagger}$ values.

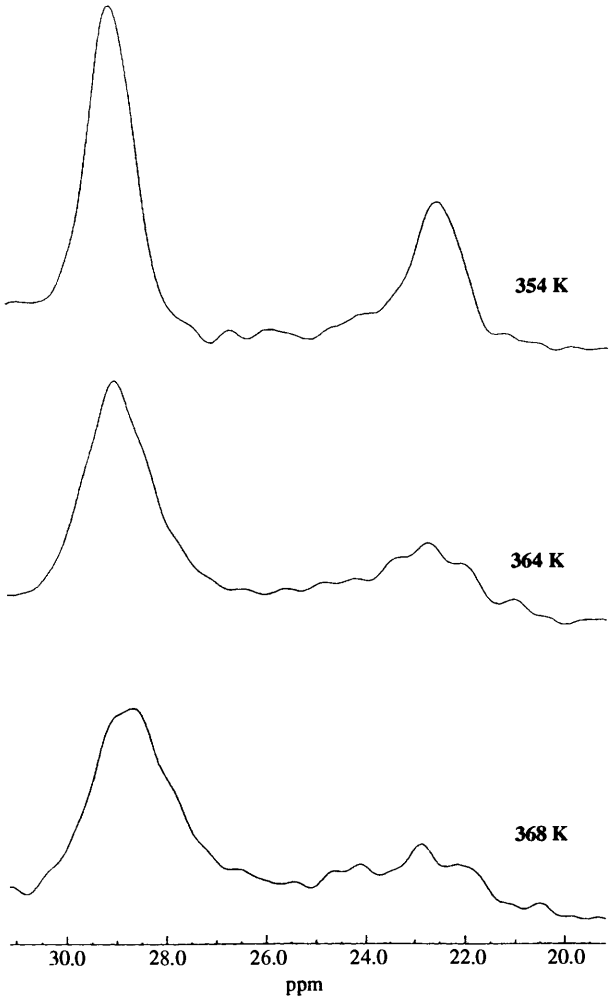

Fig. 13 Temperature variation of the ^{13}C CP/MAS NMR spectrum of the *tert*-butyl region of compound **10b** at 125.758 MHz

calculated at 293 K. Less reliable are the entropies of activation which vary between +23 and −57 J K^{-1} mol^{-1}. Although the errors on some of these values are high and although entropies of activation from NMR measurements are notoriously questionable we believe that the variation in these values is indeed a reflection of substantial differences in the entropies of activation.

It is instructive to compare our observations with the generalised predictions made at the outset of this work. In keeping with our ideas of 'least distress' every *tert*-butyl group examined showed evidence of internal rotation. The *tert*-butyl group has high local C_{3v} symmetry making it, for the purposes of this discussion, almost a conical group with bumps on. We found one example of *tert*-amyl group rotation and no examples of isopropyl group rotations. Again this accords with our ideas that *tert*-amyl might be more susceptible to rotation than isopropyl. However, contrary to our prediction that a *tert*-amyl group would have a larger activation energy than *tert*-butyl, the activation energies observed for compounds **7b** and **7c** are quite similar. We have also observed, in a related series of compounds, that an $-N^{+}Me_2Et$ (*tert*-amyl equivalent) group exhibits a very low activation energy for rotation. However, apart from these two cases we believe that our observations on *tert*-amyl groups and *tert*-amyl equivalent groups are consistent with slow *tert*-amyl group rotation and thus with our general ideas. Furthermore, we found no examples where the rates of rotation of isopropyl groups were susceptible to measurement by our methods and which we believe, therefore, to be much slower than those of *tert*-butyl groups.

Several examples of phenyl rotation were observed. Similar observations have been made previously by ourselves [5,6] and by Dobson's group and others.[7] Although the phenyl group has local C_{2v} symmetry the substantial π electron density above and below the plane of the ring makes the cross sectional area more like a thick than a thin rectangle. This moves the local symmetry in the direction of C_{4v} (cubic cross section) and helps to explain the fairly large number of such rotations now known.

We believe, after the results of these and related experiments, that the prediction of Gavezzotti and Simonetta in 1982[2] that the number of cases of large amplitude molecular motion in molecular crystals '... might be higher than is actually reported, given the fact that many investigators regard large molecular motions in crystals as an unlikely nuisance' is in fact correct. Chemists must be aware of the likelihood that there is substantial large amplitude segmental molecular motion in molecular crystals and that this is probably the normal state of affairs and not some unfortunate chance to be ignored or disregarded.

Acknowledgements

We thank the SERC for a grant that enabled the purchase of the spectrometer and for a studentship for M. R. We thank Professor Peter Bruce and Dr Phil Lightfoot for the powder diffraction determination of the structure of **8a**.[8]

References

1 I. C. Paul and D. Y. Curtin, *Acc. Chem. Res.*, 1973, **6**, 217.
2 A. Gavezzotti and M. Simonetta, *Chem. Rev.*, 1982, **82**, 1.
3 See for example: (*a*) K. D. M. Harris and A. E. Aliev, *Chem. Br.*, 1995, **31**, 132; (*b*) *Solid State NMR for Chemists*, C. A. Fyffe, CFC Press, Guelph, 1983.
4 F. G. Riddell, S. Arumugam and J. E. Anderson, *J. Chem. Soc., Chem. Commun.*, 1991, 1525.

5 F. G. Riddell, S. Arumugam, K. D. M. Harris, M. Rogerson and J. H. Strange, *J. Am. Chem. Soc.*, 1993, **115**, 1881.
6 F. G. Riddell, F. Fülöp and G. Bernáth, *J. Am. Chem. Soc.*, 1995, **117**, 2327.
7 F. G. Riddell, M. Bremner and J. H. Strange, *Magn. Reson. Chem.*, 1994, **32**, 118.
8 F. G. Riddell, P. G. Bruce, P. Lightfoot and M. Rogerson, *J. Chem. Soc., Chem. Commun.*, 1994, 209.
9 J. M. Twyman and C. M. Dobson, *J. Chem. Soc., Chem. Commun.*, 1988, 786.
10 P. J. Barrie and J. E. Anderson, *J. Chem. Soc., Perkin Trans. 2*, 1992, 2031.
11 J. B. Lambert, L. Xue and S. C. Howton, *J. Am. Chem. Soc.*, 1991, **113**, 8958.
12 J. B. Lambert, S. C. Johnson and L. Xue, *J. Am. Chem. Soc.*, 1994, **116**, 6167.
13 G. S. Harbison, D. P. Raleigh, J. Herzfeld and R. G. Griffin, *J. Magn. Reson.*, 1985, **64**, 284.
14 For a discussion of the circumstances where $T_{1\rho}$ measurements can be used to obtain dynamic information see: D. L. Vanderhart and A. N. Garroway, *J. Chem. Phys.*, 1979, **71**, 2773.
15 W. P. Rothwell and J. S. Waugh, *J. Chem. Phys.*, 1981, **74**, 2721.
16 J. Jeener, B. H. Meier, P. Bachmann and R. R. Ernst, *J. Chem. Phys.*, 1979, **71**, 4546.
17 C. L. Perrin and T. J. Dwyer, *Chem. Rev.*, 1990, **90**, 935.
18 N. M. Bortnick, L. S. Luskin, M. D. Hurwitz, W. E. Craig, L. J. Exner and J. Mirza, *J. Am. Chem. Soc.*, 1956, **78**, 4039.
19 M. Rogerson, *PhD Thesis*, St Andrews, 1995.
20 P. M. Henrichs, H. R. Luss and R. P. Scaringe, *Macromolecules*, 1989, **22**, 2731.

Paper 5/06595J
Received 6*th October* 1995
Accepted 6*th December* 1995